LOW CYCLE FATIGUE AND FRACTURE TOUGHNESS BEHAVIOUR OF A NON-MAGNETIC AUSTENITIC Cr-Mn-N STEEL

L. V. Vareda* and D. Spinelli†

In the present work, low cycle fatigue and fracture toughness behaviour of a Cr-Mn-N austenitic stainless steel used for drilcollar connections were studied. Room-temperature low cycle fatigue tests were carried out under total strain control in the range of 0.40 to 1.50% using companion specimen (CST) and incremental step (IST) methods. The J-R curves and J_{IC} values were obtained at room temperature and at 150°C by using single specimen and elastic compliance technique for crack length measurement. Cyclic softening without saturation until fracture and Massing behaviour only in IST method were observed. The fatigue life behaviour obeyed Basquin and Coffin-Manson relationships and the obtained high value of ε'_f means a significant improvement on fatigue resistance. The decrease in crack initiation fracture toughness at temperature of 150°C is proposed to be due to dynamic strain ageing effect, which impairs ductility.

INTRODUCTION

The studied material belongs to the class of high-strength non-magnetic austenitic Cr-Mn-Ni steels with high N content which are used for structural applications. According to the literature (1, 2) high-strength austenitic materials, in particular Cr-Mn-N alloys are used for drillcollar connections for deep drilling in offshore oil and gas industry. In service, these drillcollars are exposed to static and dynamic loading in corrosive environments and for all these loading conditions high strength, toughness and fatigue behaviour are required for the material. For this steel dominant strengthening mechanisms are solid solution hardening due to Cr, Mn and N and strain hardening due to grain size control during the processing of warm and cold deformation. During service, these connections are subjected to cyclic loading which could result in nucleation of crack or growth of crack-like defects. To evaluate the life to nucleated the cracks and the structural integrity of potentially flawed components the low-cycle fatigue behaviour and fracture toughness responses of the material must be characterised under 'as received' condition. This

* Department of Structural Engineering, University of São Paulo, Av. Dr. Carlos Botelho, 1465, CEP 13560-250, São Carlos, SP, Brazil. E-mail: lvvareda@sc.usp.br.

† Department of Materials Engineering, University of São Paulo, Av. Dr. Carlos Botelho, 1465, CEP 13560-250, São Carlos, SP, Brazil. E-mail: dspinell@sc.usp.br..

investigation was undertaken to evaluate low cycle fatigue properties and fracture toughness behaviour of a non-magnetic austenitic steel.

MATERIAL AND EXPERIMENTAL PROCEDURES

The investigated steel was supplied by Eletrometal S/A (Brazil) and has the designation E3949. The routine for the production process is as follows: air melted in electric arc furnace, vacuum arc remelting followed by casting into ingots, warm forged at 700°C and then water quenched. The bars with oversize dimensions are cold worked at 15%, mechanically bored out and machined for dimensions of about 9 m in length, 170 mm in OD and 75 mm in ID. The chemical composition of the steel is shown in Table 1. All investigated specimens were taken from the marginal zone and presenting grain sizes from 8 to 17 μm. The microstructure shows a matrix of fine austenitic grains and fine carbonitrides inclusions dispersed throughout the matrix.

TABLE 1 – Chemical composition (wt%) of E3949.

C	N	Mn	Cr	Ni	Nb	Si	P	S	Mo
0.040	0.22	16.74	13.22	2.24	0.21	0.35	0.034	0.002	0.50

Low cycle fatigue specimens with gauge diameter of 6.5 mm and gauge length of 14 mm were machined in longitudinal direction according to ASTM standard E606-80 (3). Room-temperature uniaxial push-pull loading low cycle fatigue (LCF) tests under total strain control were performed in air on a computer-controlled 250 kN MTS closed-loop servo-hydraulic testing machine. A sinusoidal strain waveform with strain ratio of $R_\varepsilon = -1$ at frequency of 0.5 Hz was applied. The failure condition in strain-controlled low cycle fatigue was the cusp formation in the compression portion of the stress-strain hysteresis loop. The tests were conducted with the strain amplitude limits lying between 0.40 to 1.50%. The incremental step test (IST) method was also employed to determine the cyclic stress-strain (CSS) curve. In this case, the specimen was subjected to strain blocks in which the strain amplitude increased linearly to 1.5% and then decreased.

The J-R curves for the fracture toughness determination were obtained by means of single specimen and elastic compliance technique. Additional details for the measurement of J_{IC} are specified in the ASTM E813-87 (4). The material was tested in the 'as received' condition at temperatures of 23 and 150°C. C(T) specimens with total thickness of 25.0 mm and 20% side-grooved to ensure a straight crack fronts were fabricated in the C-L crack plane orientation. All specimens were tested at load line displacement rate of 0.5 mm/min using a load line displacement control in a 250 kN computer controlled servo-hydraulic MTS testing system.

RESULTS AND DISCUSSION

Variation of the peak tensile stresses versus number of cycles of the specimens cycled with different total strain amplitudes for CST method is shown in figure 1. For all total strain amplitudes applied the material have presented stable behaviour in the first few cycles and then softening without reaching a steady state. In all cases the stress amplitude decreased rapidly towards the end of life of the specimen, due to the fast propagation of

the dominant macrocrack. As already have been reported (5) the initial stable behaviour is attributed to a minimum number of cycles which are necessary to modify the pre-existing high density of dislocations creating mobile dislocations by appropriate mechanisms of dislocation annihilation. The stage of cyclic softening occurs when the dislocation annihilation rate is greater than their generation rate, or when a rearrangement of dislocations into cells takes place, increasing the mean free path between dislocations (6).

The cyclic response of the material for the IST method is shown in figure 2. The peak tensile stresses at the highest strain amplitude of ± 1.5% in a block has been plotted versus the number of the blocks. In this method, the stress level decreased very fast, with a drop of stress amplitude of 150 MPa in the first 20 blocks. This initial fast softening was probably due to a great increase in the density of mobile dislocations created by the damage mechanism already produced in the first block of strain. It was also checked if the material exhibits Massing behaviour (7). For the CST and IST methods the hysteresis loops were taken in a half life since no stabilization were reached. Figures 3 (a) and (b) show the superimposed loops with matched lower tips for both cases. The loops recorded in the IST method exhibited ideal Massing behaviour, which was not the case in the CST method. The CSS curves obtained in CST and IST methods are compared to the monotonic stress-strain (MSS) curve, as seen in figure 4. The CSS for both methods are the locus of the tips of half-life stress-strain hysteresis loops obtained at different strain amplitudes. There was a crossover in the CSS curves obtained in both methods at strain amplitude of ±1.0%. For IST method, at strain amplitudes below ± 1.0% an appreciable cyclic softening was observed when compared to the CST method. This behaviour can be associated with increasing density of mobile dislocation created by damage produced by different levels of strain amplitude applied within a block.

Figure 5 presents the values of elastic ($\Delta\varepsilon_e/2$), plastic ($\Delta\varepsilon_p/2$) and total strain amplitudes ($\Delta\varepsilon_t/2$) plots of the material at room temperature. It was found that the Basquin relation $\Delta\varepsilon_e/2 = (\sigma'_f/E)(2N_f)^b$ and the Coffin-Manson relation $\Delta\varepsilon_p/2 = \varepsilon'_f(2N_f)^c$ fit very well the cyclic behaviour of the material. Here, σ'_f is the fatigue strength coefficient, E is Young's modulus, $2N_f$ is the number of reversals to failure, b is the fatigue strength exponent, ε'_f is the fatigue ductility coefficient, and c is the fatigue ductility exponent. The values of LCF parameters of E3949 and AISI 304LN (6) which present tensile parameters of resistance and ductility very similar are given in Table 2. It can be seen that with exception of ε'_f all others parameters are quite similar. Higher value of ε'_f means improvement of fatigue resistance of the material in all range of total strain amplitudes.

TABLE 2 – LCF parameters of E3949 and AISI 304 LN.

Material	σ'_f (MPa)	b	ε'_f (%)	c
E3949	1083	-0.056	63.20	-0.570
AISI 304LN	1032	-0.055	24.22	-0.529

The J-R curves and J_{IC} values at room temperature and 150°C can be seen in figure 6. The results show that the initiation fracture toughness of the material is greatly influenced by temperature. Decrease in fracture toughness with increase in temperature

can be explained as being due to some mechanism which impairs ductility. It has been observed that the material ultimate strength, yield strength and total elongation decrease with increasing of temperature (see figure 7). Grain boundary embrittlement caused by carbonitrides precipitation is ruled out due to short duration of test time and low temperature involved (150°C). In austenitic stainless steels another mechanism which reduces tensile strength and ductility is dynamic strain ageing, which occurs during the tensile loading of the specimen. This mechanism is caused by the interaction between dislocations and the interstitial solutes atoms (C, N) or solute pairs consisting of one interstitial and one substitutional solute atoms (Cr, Mn). The temperature domain of dynamic strain ageing depends on strain rate, grain size, type of solute, content, etc. Similar loss of toughness of a modified type AISI 316L austenitic stainless steel in the dynamic strain ageing temperature range has been reported (8).

CONCLUSIONS

1. The material presented stable behaviour in the initial few cycles of fatigue and then rapid softening until fracture without reaching saturation.

2. Massing behaviour was present in the material only in the IST method.

3. The CSS curves obtained by CST and IST methods are quite different and for IST method an appreciable softening was observed at total strain below ± 1.0 %.

4. The E3949 steel presented ε'_f value higher than AISI 304LN steel which means an improvement on fatigue resistance in all range of total strain amplitudes.

5. The decrease in crack initiation fracture toughness at temperature of 150°C is believed to be due to dynamic strain ageing effect, which impairs ductility.

REFERENCES

(1) Panzemböck, M. et al. Fatigue Fract. Engng. Mater. Struct., v.13, n.6, p.563-78, 1990.

(2) MacDonald, K.A.; Aigner, H. Engineering Failure Analysis, v.3, n.4, p.281-97, 1996.

(3) ASTM E606-80 - Standard recomended practice for constant-amplitude low cycle fatigue testing. Philadelphia, ASTM, 1991.

(4) ASTM E 813-87 - Standard test method for J_{IC}, a measure of fracture toughness. Philadelphia, ASTM, 1988.

(5) Mughrabi, H. Dislocation and Properties of Real Materials. The Institute of Metals, London, p.244-62, 1985.

(6) Raman, G.S. and Padmanabhan, K.A. Int. J. Fatigue, v.18, n.2, p.71-9, 1996.

(7) Massing,G. apud Jhansale,H.R. and Topper,T.H. In: ASTM-STP 519, p.246-70, 1973.

(8) Samuel, K.G. et al. Int. J. Pres. Ves. & Piping, v.41, p.59-74, 1990.

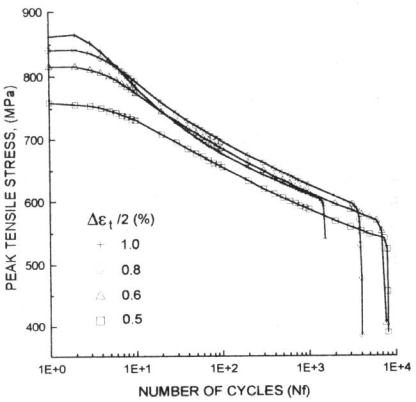

Figure 1 – Cyclic stress response versus the number of cycles in the CST method.

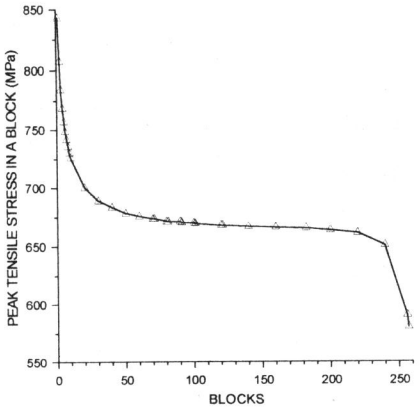

Figure 2 – Cyclic stress response versus the number of blocks in the IST method.

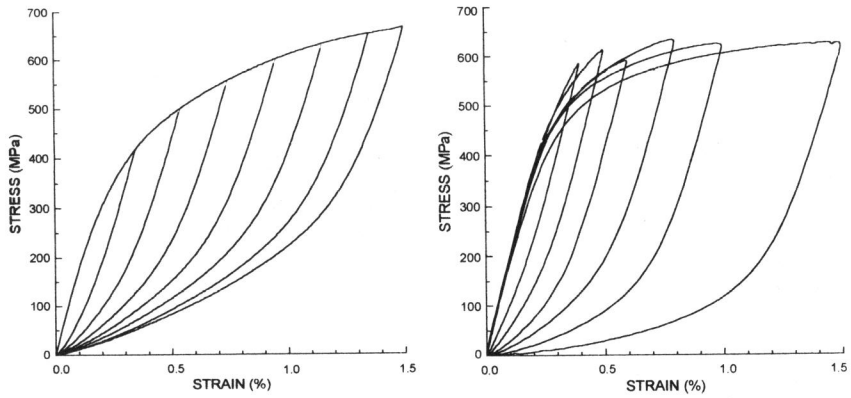

(a) (b)

Figure 3 – (a) Massing behaviour in the IST method; (b) absence of Massing behaviour in the CST method.

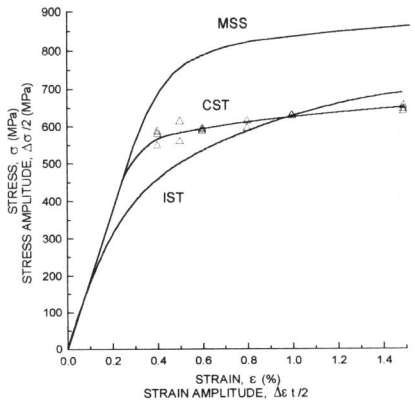

Figure 4 – MSS and CSS curves.

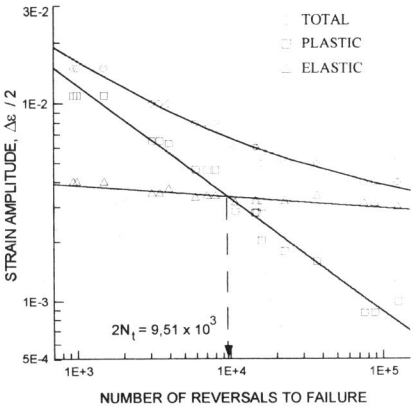

Figure 5 – Strain-life curves.

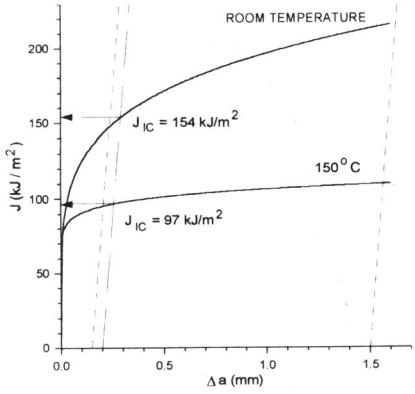

Figure 6 – J-R curves and J_{IC} values at room temperature and 150°C.

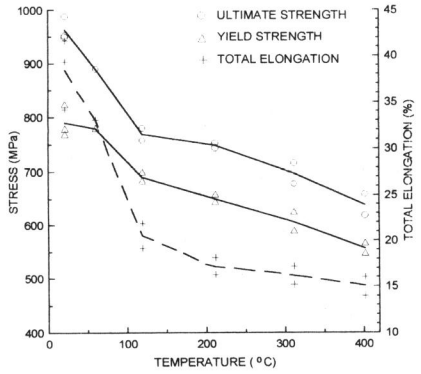

Figure 7 – Tensile properties versus temperature